Since January 2020 Elsevier has created a COVID-19 resource centre with free information in English and Mandarin on the novel coronavirus COVID-19. The COVID-19 resource centre is hosted on Elsevier Connect, the company's public news and information website.

Journal of Molecular Liquids 325 (2021) 115187

Contents lists available at ScienceDirect

Journal of Molecular Liquids

journal homepage: www.elsevier.com/locate/molliq

Charge-transfer chemistry of azithromycin, the antibiotic used worldwide to treat the coronavirus disease (COVID-19). Part I: Complexation with iodine in different solvents

Abdel Majid A. Adam [a,*], Hosam A. Saad [a], Amnah M. Alsuhaibani [b], Moamen S. Refat [a], Mohamed S. Hegab [c]

[a] Department of Chemistry, College of Science, Taif University, P.O. Box 11099, Taif 21944, Saudi Arabia
[b] Department of Physical Sport Science, Princess Nourah bint Abdulrahman University, 4545 – King Khalid Airport Unit No. 1, Riyadh 13415-7132, Saudi Arabia
[c] Deanship of Supportive Studies (D.S.S.), Taif University, P.O. Box 11099, Taif 21944, Saudi Arabia

ARTICLE INFO

Article history:
Received 19 October 2020
Received in revised form 14 December 2020
Accepted 22 December 2020
Available online 26 December 2020

Keywords:
Charge–transfer
Iodine
Azithromycin
Tri–iodide ion
Solvent effect

ABSTRACT

Around the world, the antibiotic azithromycin (AZM) is currently being used to treat the coronavirus disease (COVID-19) in conjunction with hydroxychloroquine or chloroquine. Investigating the chemical and physical properties of compounds used alone or in combination to combat the COVID-19 pandemic is of vital and pressing importance. The purpose of this study was to characterize the charge transfer (CT) complexation of AZM with iodine in four different solvents: CH_2Cl_2, $CHCl_3$, CCl_4, and C_6H_5Cl. AZM reacted with iodine at a 1:1 M ratio (AZM to I_2) in the $CHCl_3$ solvent and a 1:2 M ratio in the other three solvents, as evidenced by data obtained from an elemental analysis of the solid CT products and spectrophotometric titration and Job's continuous variation method for the soluble CT products. Data obtained from UV–visible and Raman spectroscopies indicated that AZM strongly interacted with iodine in the CH_2Cl_2, CCl_4, and C_6H_5Cl solvents by a physically potent n→σ* interaction to produce a tri-iodide complex formulated as $[AZM{\cdot}I^{+}]I_3^{-}$. XRD and TEM analyses revealed that, in all solvents, the AZM-I_2 complex possessed an amorphous structure composed of spherical particles ranging from 80 to 110 nm that tended to aggregate into clusters. The findings described in the present study will hopefully contribute to optimizing the treatment protocols for COVID-19.

1. Introduction

Robert Mulliken introduced a new concept through his investigations of Lewis acid-base interactions in 1969, this concept is the electron donor-acceptor interactions or charge transfer (CT) interactions. Thereafter, the concept of CT interactions was widely disseminated by Roy Foster. Foster described the importance of CT complexes in several physicochemical processes such as paramagnetism, semiconductivity, photoconductivity, and in biological processes [1–6]. CT interactions have been used in dendrimers, photocatalysts, optical communication, non-linear optical materials, optoelectronics, organic semiconductors, biosensors, electrical conductors, organic semiconductors, organic solar cells, and solar energy storage devices [7–47]. Complexation through the CT mechanism enables a long list of applications including studying binding mechanisms of pharmaceutical receptors, studying the pharmacodynamics and thermodynamics of molecules, and anti-inflammatory, antitumor, and antimicrobial studies [48–66]. Given the constant increase in the number and types of applications involving CT complexation and the concomitant increase in relevance and attention, extensive research efforts have been dedicated to characterizing the crystallographic, thermodynamic, kinetic, photophysical, and spectral characteristics of CT complexation [67–119]. New CT complexations between π-conjugated organic ring molecules or π-electron-deficient acceptors with π-electron-rich donors represent an important approach to developing optoelectronic, light-emitting superconductor and conductor devices with valuable properties such as long-persisting luminescence, superconductivity, and high electrical conductivity [120–131].

The donor used in this study was azithromycin (AZM, $C_{38}H_{72}N_2O_{12}$, 748.98 g/mol; Scheme 1) a well-tolerated, effective, broad-spectrum antibiotic. AZM was approved by the FDA for enteric infections like typhoid, genitourinary infections like chlamydia, and viral respiratory tract infections like influenza and pneumonia [132–135]. The great importance of AZM as an antibiotic arises from it being the most suitable macrolide in a possible therapeutic combination and its recent use in the treatment protocol against severe acute respiratory syndrome coronavirus 2 (SARS-CoV-2). On December 9, 2019, the first case of this syndrome was reported in Wuhan, China; thereafter, it spread swiftly throughout China and around the globe [136]. By early March 2020, the World Health

* Corresponding author at: Department of Chemistry, College of Science, Taif University, P.O. Box 11099, Taif 21944, Saudi Arabia.
E-mail address: majidadam@tu.edu.sa (A.M.A. Adam).

https://doi.org/10.1016/j.molliq.2020.115187
0167-7322/

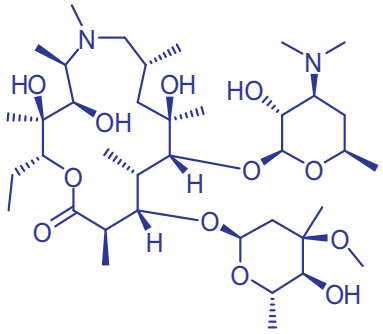

Scheme 1. Structure of the AZM molecule.

Organization (WHO) declared the coronavirus disease (COVID-19) outbreak a pandemic [137]. The severity and rapid spread of COVID-19 have resulted in significant mortality and morbidity around the world and in a global rush to find an effective antiviral treatment to conquer this pandemic, treat patients, and reduce the risk of complications [138]. Data reported in the literature indicate that in recent trials, AZM showed clinical efficacy as a potential treatment for COVID-19 in combination with hydroxychloroquine or chloroquine [139–144]. The acceptor used in this study is molecular iodine (I_2). Molecular iodine is a typical σ-acceptor with high molecular polarizability among halogens and an electron affinity equal to 3.059 eV. Extensive research efforts have focused on the complexation of iodine with different types of electron *n*- and π- donors to form both weak and strong CT complexes. It forms a large number of complexes with a wide variety of heterocyclic, aliphatic, and aromatic molecules [145–167]. The purpose of this study was to characterize the CT interaction of AZM with iodine in four different solvents: CH_2Cl_2, $CHCl_3$, CCl_4, and C_6H_5Cl.

2. Experimental

2.1. Chemicals and measurements

All chemicals were procured from commercial chemical sources. The main chemicals used in this study were AZM powder ($C_{38}H_{72}N_2O_{12}$; 748.98 g/mol; ≥ 98% Merck KGaA, Germany), iodine crystals (I_2; 253.81 g/mol; ≥ 99.8% Sigma-Aldrich, USA), and the following solvents (Merck KGaA, Germany): dichloromethane (CH_2Cl_2; ≥ 99.8%), trichloromethane ($CHCl_3$; ≥ 99%), tetrachloromethane (CCl_4; ≥ 99.5%), and chlorobenzene (C_6H_5Cl; 99.8%). Safety precautions included using gloves, eye shields, and dust masks. Elemental analyses of nitrogen, hydrogen, and carbon are reported in percentages and were generated using a Perkin-Elmer CHN Microanalyzer (Model PE 2400 series II). The HACH LANGE GmbH UV/VIS Spectrophotometer (Model DR6000 Benchtop) was used to record the UV–visible spectra and spectrophotometric measurements in absorption mode from 200 nm to 800 nm with 1.0-cm path length optical quartz cells. A Shimadzu Fourier Transform Infrared Spectrophotometer (FT-IR, Model IR Tracer-100) was used to collect the FT-IR spectra in transmission mode from 400 cm^{-1} to 4000 cm^{-1}. A Bruker Fourier Transform Raman Spectrophotometer (Model MultiRAM Stand Alone; 50 mW laser) was used to collect the FT-Raman spectra in Raman intensity over mode from 50 cm^{-1} to 3600 cm^{-1}. The microscopic morphology of the complexes prepared in the different solvents was investigated using the JEOL Transmission Electron Microscope (TEM; Model JEM-1200EX II). TEM micrographs were collected at 100 kV. A Malvern Panalytical's X-ray Powder Diffractometer (Model X'Pert^3 MRD) was used to collect the XRD spectra from a diffraction angle (2θ) of 5° to 80° at a radiation wavelength (λ) of 0.154056 nm.

2.2. Stoichiometry of the AZM-I_2 interaction

Three methods were used to determine the stoichiometry of the AZM-I_2 interaction: *i)* Job's continuous variation method [168], *ii)* spectrophotometric titration [169] of the soluble CT product, and *iii)* elemental analysis of the solid CT product. Standard solutions of AZM and I_2 at a concentration of 5.0×10^{-4} M were prepared by dilution in the appropriate solvent (CH_2Cl_2, $CHCl_3$, CCl_4, and C_6H_5Cl) from their stock solutions (10×10^{-3} M). All stock and standard solutions were stored in the dark at all times. To determine the wavelength (nm) of the CT band (λ_{CT}), the UV–visible spectra of the CT complex as well as the free components (AZM and I_2) were scanned between 200 and 800 nm at room temperature in the appropriate solvent.

2.2.1. Job's continuous variation method

A series of 10 solutions in volumetric flasks (20 mL) containing AZM and I_2 at varied molar fractions ($C_{AZM} + C_{iodine}$) was prepared in the appropriate solvent. The total concentration in each flask was kept constant. The 10 solutions were left at room temperature for 10 min to allow the reaction to reach equilibrium. Then, the absorbances of the developed colors were measured at λ_{CT} against a similarly treated blank reagent. The measured absorbances were plotted against the corresponding molar fraction of iodine calculated using the equation: $\chi_{iodine} = C_{iodine}/(C_{AZM} + C_{iodine})$. The molar ratio of the AZM-I_2 interaction was determined from the resulting plot.

2.2.2. Spectrophotometric titration

A series of 10 solutions in volumetric flasks (20 mL) containing AZM and I_2 with varied AZM to iodine molar ratios ranging from 1:4 to 4:1 were prepared in the appropriate solvent. The concentration of AZM in each flask was kept constant, while the concentration of I_2 varied. The 10 solutions were kept at room temperature for 10 min to allow the reaction to reach equilibrium. Then, the absorbance of each solution was measured at λ_{CT} against a similarly treated blank reagent. The absorbance of each solution was plotted as a function of the corresponding iodine volume in the solution. The molar ratio of the AZM-I_2 interaction was determined from the resulting plot and compared with that obtained using Job's continuous variation method.

2.3. Synthesis of the AZM-I_2 complex

One mmol of AZM and two mmol of iodine were separately dissolved in 25 mL of CH_2Cl_2 solvent. The two solutions were mixed and stirred thoroughly for 10 min on a magnetic stir plate at room temperature. The resulting light-brown-colored solution was incubated at 4 °C for 24 h to fully complete the precipitation process. The resultant brown-colored precipitate was filtered from the solvent using Whatman 42 grade filter paper and recrystallized in the CH_2Cl_2 solvent to increase its purity. One day later, the resulting precipitate was filtered from the solvent. The recrystallized product was washed three times with the least possible volume of CH_2Cl_2 solvent and the collected product was vacuum dried over $CaCl_2$ (anhydrous) in a desiccator at room temperature for 48 h [160–163,170–173]. This procedure was then repeated in the other solvents ($CHCl_3$, CCl_4, C_6H_5Cl). To verify the resultant AZM-I_2 product, a small amount was dissolved in CH_2Cl_2 solvent to which a few drops of aqueous HCl acid was added. The iodine color was restored faintly, supporting the formation of the desired product. The iodine content in the product was determined by iodimetry titrations.

3. Results and discussion

3.1. Soluble and solid CT products

The soluble CT product was generated by mixing the AZM solution in the appropriate solvent (CH_2Cl_2, $CHCl_3$, CCl_4, or C_6H_5Cl) at a

Fig. 1. Strong color change upon mixing iodine (*far left*; *violet*) with AZM (*middle; colorless*) to produce the AZM-I_2 CT complex (*far right*; *brown*) in the CH_2Cl_2 solvent.

concentration of 5.0×10^{-4} M with the iodine solution in the same solvent at the same concentration. The AZM solutions, regardless of solvent, were colorless, while the iodine solution in all of the solvents had a violet color. The resulting soluble CT products had an intense brown color in the CH_2Cl_2, CCl_4, and C_6H_5Cl solvents; this type of color change resulted from the π-π interactions and provides evidence of a strong CT interaction. Fig. 1 shows the prominent change in color upon mixing AZM with iodine in the CH_2Cl_2 solvent (as an example). The solid CT product was generated by reacting 1 mmol of AZM (white) with 2 mmol of iodine (dark grey) in the appropriate solvent (CH_2Cl_2, $CHCl_3$, CCl_4, or C_6H_5Cl). As an example, this interaction in the CH_2Cl_2 solvent resulted in a strong color change in forming the brown-colored solid CT, as pictured in Fig. 2. The strong change in color resulting from the complexation of AZM with iodine into either soluble or solid products confirms that the CT interaction between the two components took place in all of the solvents used.

3.2. CT absorptions

The electronic absorption spectrum of free AZM (5.0×10^{-4} M), free iodine (5.0×10^{-4} M), and the CT complex resulting from mixing the two solutions in the CH_2Cl_2, $CHCl_3$, CCl_4, or C_6H_5Cl solvents were scanned in UV–visible region (Fig. 3). Characteristic spectral changes were observed upon the formation of the CT complex in each solvent, as seen in Fig. 3, this figure calls for the following observations:

(i) Free AZM displays no detectable absorption band in any solvent.
(ii) Free iodine displays a weak yet broad absorption band ranging from ~430 nm to ~620 nm in all solvents, with maximum absorption observed at 505 nm for the CH_2Cl_2 and C_6H_5Cl solvents, 510 nm for the $CHCl_3$ solvent, and 517 nm for the CCl_4 solvent. This is the characteristic "iodine band" arising from the $4\pi\rightarrow10\sigma^*$ electronic transition.
(iii) The CT interaction between AZM and iodine in the $CHCl_3$ solvent strongly affected the characteristic iodine band, which became very broad and strong in this solvent and was unnoticeable in the other solvents.
(iv) The CT interaction between AZM and iodine in the CH_2Cl_2, CCl_4, and C_6H_5Cl solvents gave rise to two new very strong, broad absorption bands. The first band was observed at 297 nm in all three solvents, while the second band was located at 364 nm in the CH_2Cl_2 and C_6H_5Cl solvents and 372 nm in the CCl_4 solvent.
(v) The absorption band observed at 297 nm was caused by the iodide ion (I^-). This iodide ion was associated with the formation of an inner complex formulated as $[AZM\cdot I^+]I^-$.
(vi) The absorption band at ~364–372 nm was caused by the rapid formation of a tri-iodide ion (I_3^-) in solution from the CT complexation. This blue-shifted iodine band is the characteristic absorption band of the asymmetric tri-iodide ion (I_3^-) resulting from the formation of the AZM-I_2 complex [157,160,162]. The iodine band observed in the free iodine solution (505 nm for the CH_2Cl_2 and C_6H_5Cl solvents and 517 nm for the CCl_4 solvent) hypsochromically shifted to 364–372 nm upon the addition of the AZM solution. This blue-shifted iodine band could reflect a perturbation in the iodine's $10\sigma^*$ molecular orbital due to a repulsive interaction between the iodine and AZM [147].

3.3. Stoichiometry profile

3.3.1. Soluble CT products

The stoichiometry of the AZM-I_2 interaction was verified using Job's continuous variation method and the spectrophotometric titration method for the soluble CT products synthesized in each solvent. Fig. 4 illustrates the curves generated by applying both methods. In Job's continuous variation method, plotting the molar fractions of iodine on the (x) axis against the absorbances at λ 510 ($CHCl_3$), 364 (CH_2Cl_2 and

Fig. 2. Representative image of **(A)** free AZM (white) and **(B)** the solid AZM-I_2 CT complex (brown).

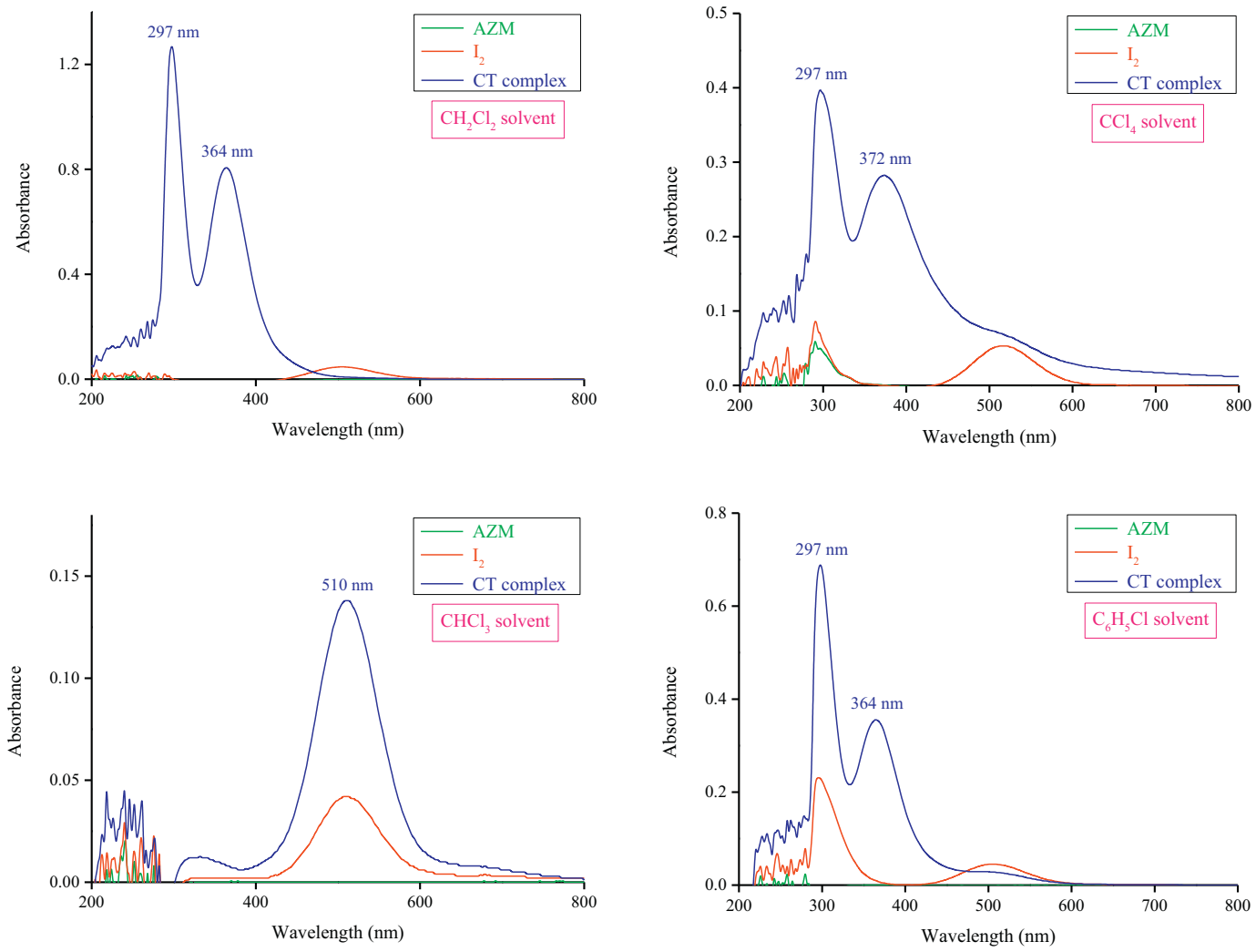

Fig. 3. Electronic absorption spectra of the AZM donor (5.0×10^{-4} M), the iodone acceptor (5.0×10^{-4} M), and the resulting AZM-I_2 complex in CH_2Cl_2, CH_3Cl, CCl_4 and C_6H_5Cl solvents.

C_6H_5Cl), or 372 nm (CCl_4) of the solutions prepared with different AZM to iodine molar fractions on the (y) axis gave a symmetrical curve (Fig. 4). For this curve, the maximum absorbance corresponded to a molar fraction of 0.50 for the complex prepared in the $CHCl_3$ solvent and 0.33 for the complexes prepared in the other solvents. These molar fractions reflect the formation of a 1:1 AZM-I_2 complex in the $CHCl_3$ solvent and a 1:2 AZM-I_2 complex in the CH_2Cl_2, CCl_4, and C_6H_5Cl solvents. In the spectrophotometric titration, plotting iodine volumes (in mL) on the (x) axis against the absorbances at λ 510 ($CHCl_3$), 364 (CH_2Cl_2 and C_6H_5Cl), or 372 nm (CCl_4) of solutions prepared with different AZM to iodine molar ratios on the (y) axis gave two straight lines (Fig. 4). The intersection of these two straight lines corresponded to an iodine volume of 1.0 mL for the complex prepared in the $CHCl_3$ solvent and 2.0 mL for the complexes prepared in the other solvents. These volumes correspond to an AZM to iodine ratio of 1:1 in the $CHCl_3$ solvent and 1:2 in the other solvents.

3.3.2. Solid CT products

The stoichiometry of the AZM-I_2 interaction was verified by the elemental analysis of the solid CT products. The elemental results for the solid CT product prepared in the $CHCl_3$ solvent were: $C_{38}H_{72}N_2O_{12}I_2$ (1002.79 g/ mol) observed % (calculated %) for C, 45.25 (45.47); H, 7.37 (7.18); N, 3.05 (2.79); I, 25.12 (25.31). The elemental results for the solid CT products prepared in the CH_2Cl_2, CCl_4, and C_6H_5Cl solvents were: $C_{38}H_{72}N_2O_{12}I_4$ (1256.6 g/ mol) observed % (calculated %) for C, 36.08 (36.29); H, 5.92 (5.73); N, 2.50 (2.23); I, 40.18 (40.40). These results suggested that the AZM-I_2 interaction in the $CHCl_3$ solvent formed a complex with the formula AZM·I_2 at a molar ratio of 1:1 and, in the other three solvents, complexes with the formula $[AZM\cdot I^+]I_3^-$ were generated at a molar ratio of 1:2.

3.4. CT interaction mechanism

The UV–visible spectral data support the strong interaction between AZM and I_2 achieved through CT complexation in the CH_2Cl_2, CCl_4, and C_6H_5Cl solvents. In these solvents, CT complexation proceeded through the formation of an asymmetric tri-iodide ion (I_3^-), as evidenced by the appearance of a band at 364–372 nm that is characteristic of the I_3^- ion. The formation mechanism of the I_3^- ion involves three steps [1,157–162]:

Step 1:

One AZM molecule fast reacted with one I_2 molecule to form an initially associative outer-sphere complex according to the following equation: AZM + I_2 → AZM· I_2.

Step 2:

The resulting outer-sphere complex (AZM· I_2) slowly transferred into a dissociative inner-sphere complex according to the following equation: AZM·I_2 → $[AZM\text{-}I]^+I^-$.

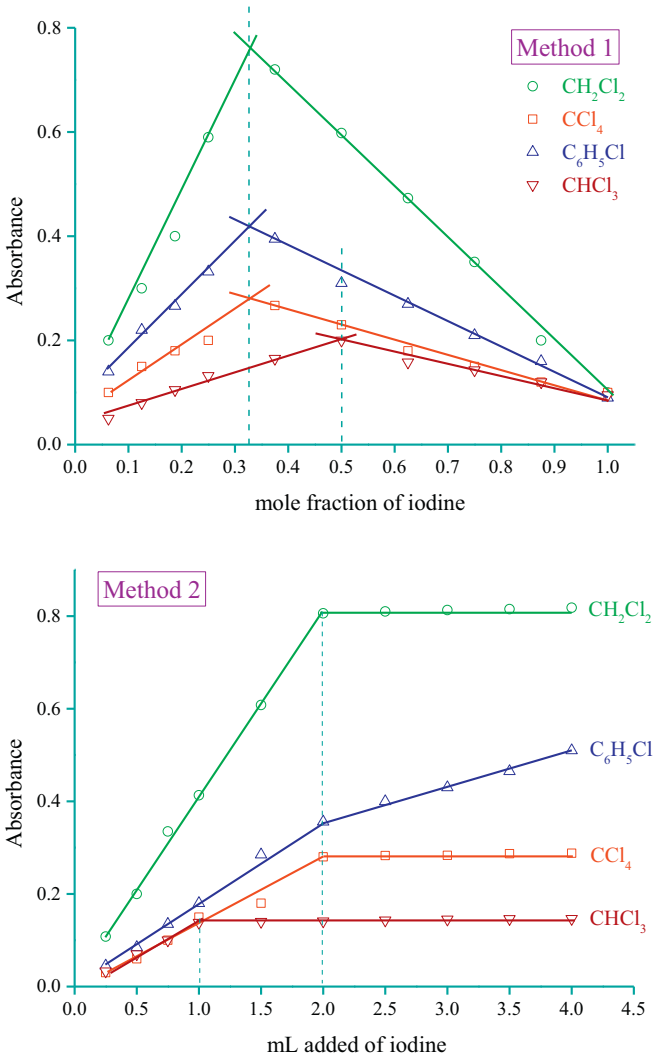

Fig. 4. Stoichiometry of the interaction between AZM and I_2 in solution-state determined by *Method 1*: Job's continuous variation, and *Method 2*: spectrophoometric titration.

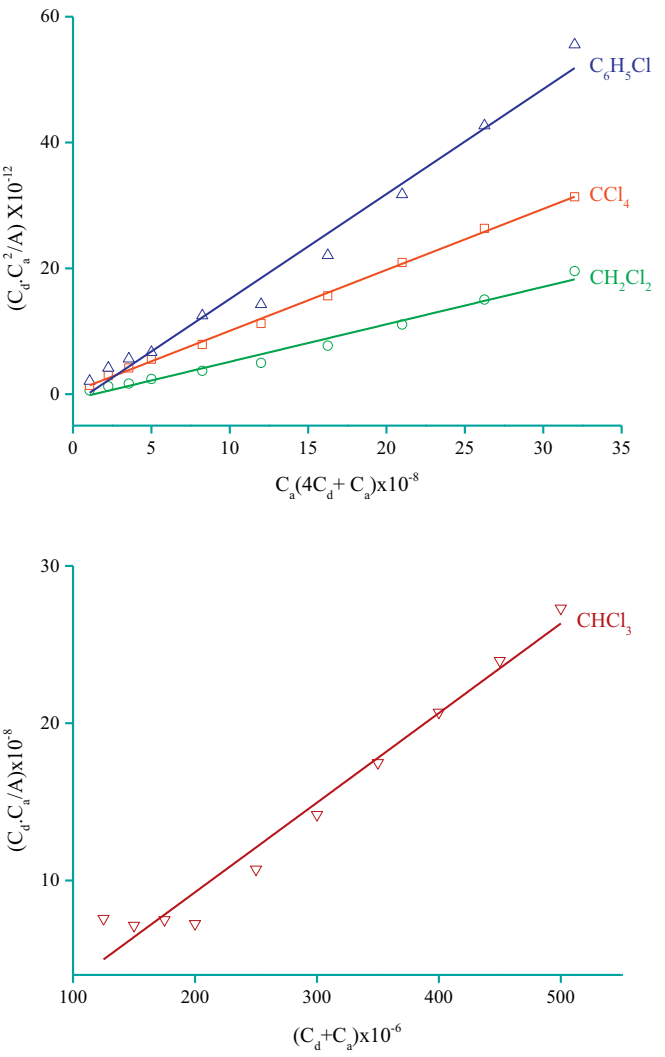

Fig. 5. The 1:1 and 1:2 Benesi-Hildebrand plots of the AZM–I_2 complex prepared in different solvents.

Step 3:

The $[AZM\text{-}I]^+I^-$ complex rapidly associated with another I_2 molecule forming the tri-iodide complex: $[AZM\text{-}I]^+I^- + I_2 \rightarrow [AZM\text{-}I]^+ + I_3^-$.

The absorption band characteristic of the I_3^- ion was not detected when the CT complexation proceeded in the $CHCl_3$ solvent. In this solvent, AZM and I_2 reacted to form a CT complex formulated as $AZM \cdot I_2$.

3.5. Spectroscopic parameters

Spectroscopic parameters like the standard free energy ($\Delta G°$), the resonance energy (R_N), the oscillator strength (f), the ionization potential (I_P), the transition dipole moment (μ), the energy of interaction (E_{CT}), the formation constant (K_{CT}), the molar extinction coefficient (ε_{max}), and the dissociation energy (W) were calculated for the AZM-I_2 complex in each solvent at room temperature using the 1:1 and 1:2 Benesi–Hildebrand plots (Fig. 5) and equations described elsewhere [174–184]. The spectroscopic parameters for the AZM-I_2 complex in each solvent are tabulated in Table 1. The AZM-I_2 complex had a high K_{CT} in the CH_2Cl_2, CCl_4, and CH_5Cl solvents, suggesting that this complex is highly stable and strongly bounded [185]. The value of $\Delta G°$ was negative, suggesting that the complexation between AZM and I_2 in all solvents was reasonably stable, spontaneous, and exothermic [186]. The AZM-I_2 complex exhibited the highest values of K_{CT} and $\Delta G°$ in the CCl_4 solvent compared with the other three solvents. The values of these two parameters for the complex decreases in the solvents in the following order: $CCl_4 > C_6H_5Cl > CH_2Cl_2 > CHCl_3$.

Table 1
Spectroscopic parameters of the AZM-I_2 complex at 298 K according to solvent.

Property	Value			
	CH_2Cl_2	CCl_4	C_6H_5Cl	CH_3Cl
λ_{max} (nm)	364	364	372	510
Formation constant; K_{CT} (L mol^{-1})	74×10^6	257×10^6	107×10^6	2.7×10^6
Free energy change; ΔG° (kJ mol^{-1})	-4.49×10^4	-4.80×10^4	-4.58×10^4	-3.67×10^4
Extinction coefficient; ε_{max} (L mol^{-1} cm^{-1})	16.8×10	10.3×10^3	6×10^3	175×10^3
Resonance energy; R_N	0.42	0.31	0.21	0.62
Energy of interaction; E_{CT} (eV)	3.42	3.34	3.42	2.44
Ionization potential; I_p (eV)	9.96	9.87	9.95	8.76
Dissociation energy; W (eV)	3.48	3.47	3.47	3.26
Oscillator strength; f	1.209	0.557	0.431	7.583
Dipole moment; μ (Debye)	3.06	2.10	1.83	9.06
Correlation coefficient; r	0.9909	0.9991	0.9906	0.9853

3.6. Vibrational spectroscopies

3.6.1. Infra-red spectroscopy

Fig. 6 contains the FT-IR spectra of free AZM and the CT complex prepared in the CH_2Cl_2 solvent collected from 4000 to 400 cm^{-1}. The characteristic IR bands of free AZM listed in Table 2 are:

3.6.1.1. O-H vibrations. The O-H groups of the AZM molecule gave rise to three vibrational modes: out-of-plane bending, in-plane bending, and stretching vibrations; these were observed at 731, 898, and 3496–3238 cm^{-1}, respectively [187].

3.6.1.2. CH_3 and CH_2 vibrations. The bands corresponding to the four vibrational modes of methyl (CH_3) groups, $\nu_{as}(CH_3)$, $\nu_s(CH_3)$, $\delta_{sciss}(CH_3)$, and $\delta_{rock}(CH_3)$, were located at 2972, 2887, 1450, and 832 cm^{-1}, respectively. The bands resulting from the six vibrational modes of methylene (CH_2) groups, $\delta_{twist}(CH_2)$, $\delta_{wag}(CH_2)$, $\delta_{rock}(CH_2)$, $\delta_{sciss}(CH_2)$, $\nu_s(CH_2)$, and $\nu_{as}(CH_2)$, appeared at 560, 794, 1260, 1374, 2830, and 2932 cm^{-1}, respectively [188–190].

3.6.1.3. C=O vibrations. The two characteristic absorption bands resulting from C=O vibrations were observed at 1718 and 1660 cm^{-1} due to the $\nu_{as}(C{=}O)$ and $\nu_s(C{=}O)$ vibrational modes, respectively. The former (asymmetric mode) appeared as a sharp, medium-strong band, while the latter (symmetric vibrational mode) was broad and weak.

3.6.1.4. C-N, C-O, and C-C vibrations. The bands resonating at 1175, 1088, 1040, and 984 cm^{-1} were associated with the ν_{as}(C-N), ν_s(C-N), ν(C-O), and ν(C-C) vibrational modes, respectively [191]. Among these, the band resulting from the ν(C-O) vibration was very strong and sharp.

The FT-IR spectrum of the CT complex contained absorption bands at 3355, 1720, 1626, 1169, 1046, 1000, and 950 cm^{-1}, which originated, respectively, from the stretching vibrations of ν(O-H), $\nu_{as}(C{=}O)$, $\nu_s(C{=}O)$, ν_{as}(C-N), ν_s(C-N), ν(C-O), and ν(C-C). The IR spectra of the complex contained all of the principle bands for the AZM molecule with several complexation-associated changes in their intensities. The most notable change was observed in the ν(C-O) and ν(O-H) vibrations; these two bands were most affected by the CT complexation with iodine. The complexation with iodine decreased the intensity of the band resulting from the C-O bonds with a slight shift in position from 1040 to 1000 cm^{-1}. The shape and position of the band originating from the ν(O-H) vibration was also affected; this band became wider and shifted from 3486 cm^{-1} to 3355 cm^{-1} upon complexation. The broadening indicates the formation of intermolecular H-bonding between the O-H group and tri-iodide ion (I_3^-) in the complex.

The concurrent broadening and shift observed for the band characteristic of the ν(O-H) vibration suggested that one or more of the O-H groups in the AZM molecule may undergo H-broadening and participate in the CT interaction with the I_2 molecule.

Table 2
FT-IR frequencies with their tentative vibrational assignments for free AZM and the CT complex prepared in the CH_2Cl_2 solvent.

Wavenumber (cm^{-1})		Mode of vibration
Free AZM	CT complex	
3486, 3238	3355	ν(O-H)
2972	2965	$\nu_{as}(CH_3)$
2932	2930	$\nu_{as}(CH_2)$
2887	2883	$\nu_s(CH_3)$
2830, 2782	–	$\nu_s(CH_2)$
1718	1720	$\nu_{as}(C{=}O)$
1660	1626	$\nu_s(C{=}O)$
1450	1455	$\delta_{sciss}(CH_3)$
1374	1378	$\delta_{sciss}(CH_2)$
1260	1255	$\delta_{rock}(CH_2)$
1175	1169	ν_{as}(C-N)
1088	1046	ν_s(C-N)
1040	1000	ν(C-O)
984	950	ν(C-C)
898	893	δ(O-H) in-plane bending
832	–	$\delta_{rock}(CH_3)$
794	798	$\delta_{wag}(CH_2)$
731	750	δ(O-H) out-of-plane bending
560	575	$\delta_{twist}(CH_2)$

3.6.2. Raman spectroscopy

Valuable information on the structural features of polyiodide anions can be obtained using Raman spectroscopy. Maki and Forneris [192] reported that the bands observed at 161 and 111 cm^{-1} in the Raman spectrum of I_3^- correspond to the asymmetric and symmetric stretching vibrations, respectively. The laser Raman spectrum of the AZM-I_2 complex prepared in the CH_2Cl_2 solvent, presented in Fig. 7, contained three bands at 70, 108, and 156 cm^{-1} reflective of the $\delta(I_3^-)$, ν_s(I-I), and ν_{as}(I-I) modes, respectively [192–195]. These three bands are characteristic of the tri-iodide ion (I_3^-), which confirmed that the CT

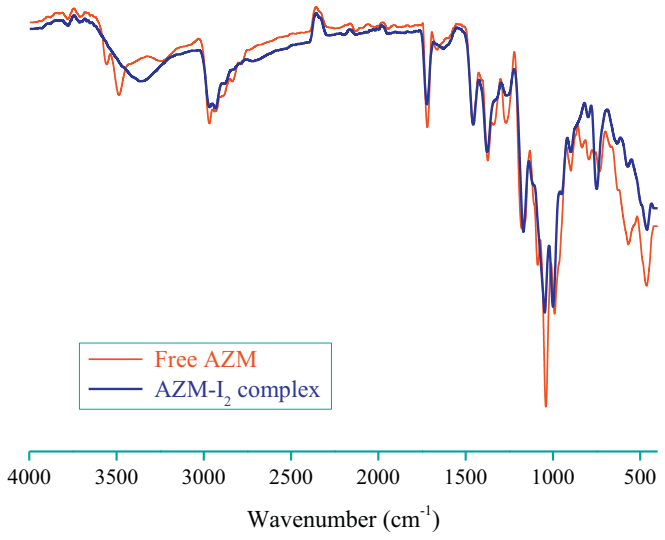

Fig. 6. IR spectra of the free AZM, and the resultant CT complex in CH_2Cl_2 solvent.

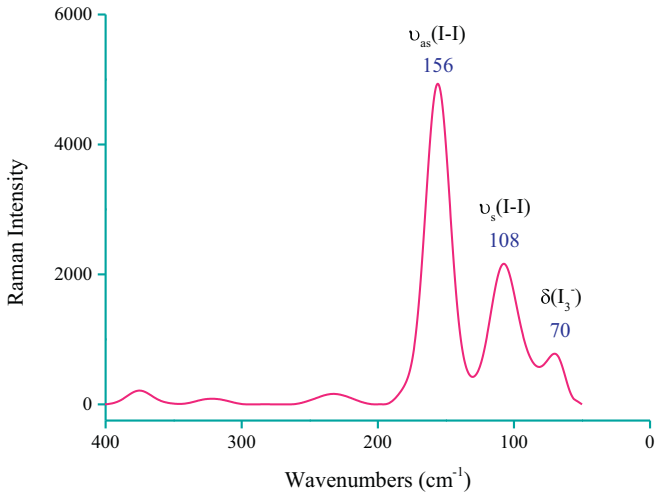

Fig. 7. Raman spectrum of AZM–I_2 complex in CH_2Cl_2 solvent.

complexation between AZM and I_2 in the CH_2Cl_2 solvent proceeded through the formation of an asymmetric tri-iodide ion (I_3^-), thus supporting the data obtained by UV–visible spectroscopy. According to group theory, the tri-iodide ion (I_3^-) may be nonlinear (belonging to the C_{2v} point group) or linear (belonging to the D_h point group). An I_3^- ion with C_{2v} symmetry displays three vibrational motions: $\delta(I_3^-)$; A_1, ν_s(I-I); B_2, and ν_{as}(I-I); A_1; these three motions are active in IR and Raman spectroscopy near 80, 100–120, and 130–155 cm^{-1}, respectively [196–202].

3.7. Morphology of the solid CT products

3.7.1. Powder XRD profiles

The solid CT products prepared in the CH_2Cl_2, $CHCl_3$, CCl_4, and C_6H_5Cl solvents were examined by powder XRD spectroscopy to determine the framework structure and phase purity of these products. The solid products were ground into powders and scanned from a diffraction angle (2θ) of 5° to 80°; the resultant spectra are presented in Fig. 8. The AZM-I_2 complexes prepared in the CH_2Cl_2, CCl_4, and C_6H_5Cl solvents exhibited similar XRD patterns marked by one broad peak ranging from 2θ 13° to 30° and centered at approximately 20°. The profile of the complex prepared in the $CHCl_3$ solvent displayed a much broader peak ranging from 2θ 17° to 50° centered at a 2θ of approximately 37°. The absence of a sharp and intense diffraction pattern suggests that the solid CT products possess an amorphous structure.

3.7.2. TEM imaging

The solid CT products prepared in the CH_2Cl_2, $CHCl_3$, CCl_4, and C_6H_5Cl solvents were visualized with TEM to observe both the shape and size of their particles. Figs. S1, S2, S3, and S4 contain the TEM images of the AZM-I_2 complex prepared in the CH_2Cl_2, $CHCl_3$, CCl_4, and C_6H_5Cl solvents, respectively. The TEM images were captured at 6000× to 30,000× magnification with an accelerating voltage of 100 kV. TEM imaging revealed the high similarity in the particles' morphology even when generated in different solvents. The particles from the complexes generated in every solvent were spherical, ranged in diameter from 80 to 110 nm, and tended to aggregate into big clusters.

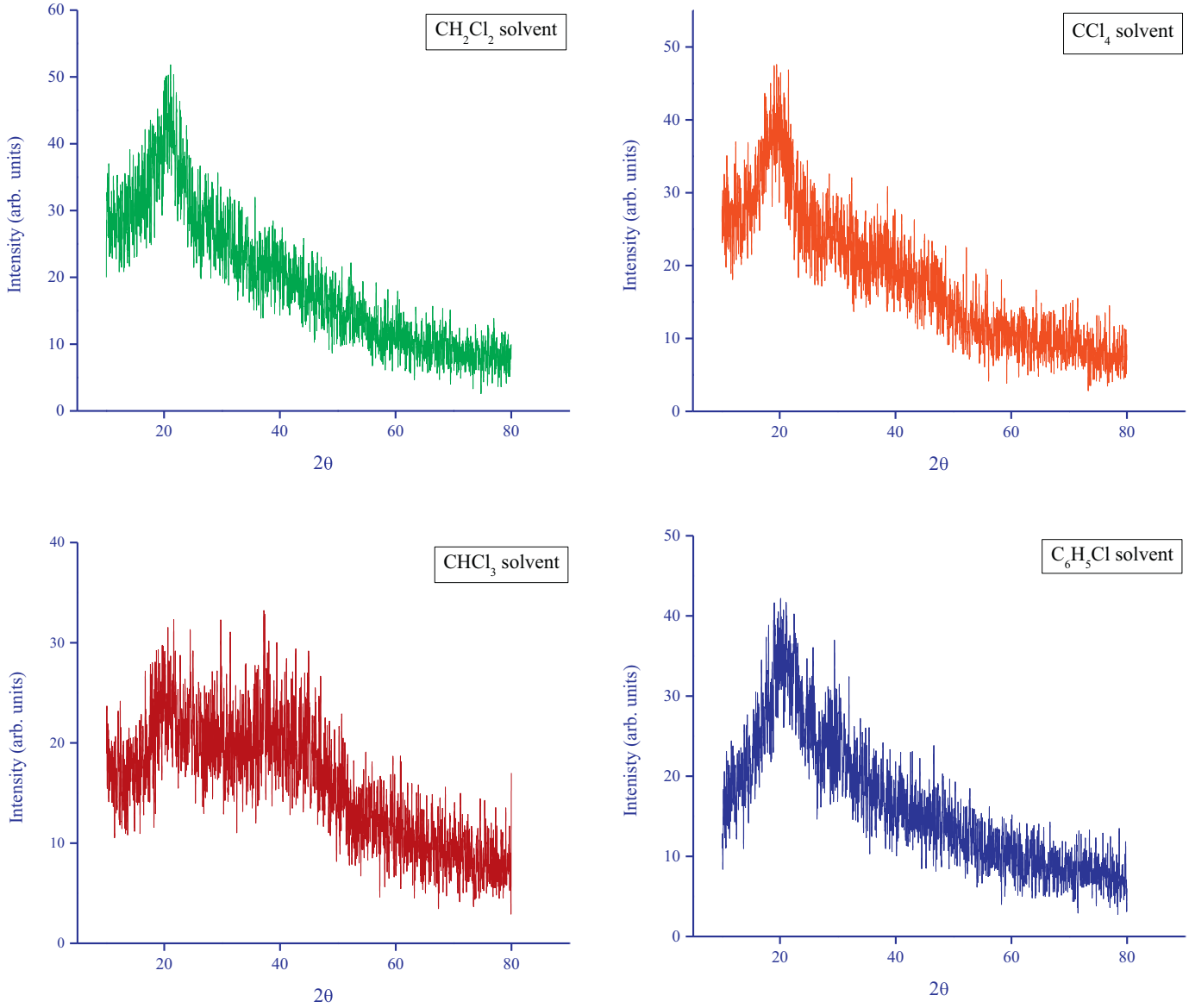

Fig. 8. XRD spectra of the solid CT products prepared in CH_2Cl_2, CH_3Cl, CCl_4 and C_6H_5Cl solvents.

4. Conclusions

The most pressing issue facing the world in 2020 and 2021 is finding a cure or vaccine for COVID-19. One of the current treatment protocols, subject to continuous examination and evaluation, is based on the antibiotic azithromycin (AZM) in combination with hydroxychloroquine or chloroquine. Providing new insight into the chemistry of this antibiotic may help researchers to improve such treatment protocols. Here we describe the CT interaction between AZM as a donor and iodine as an acceptor in four different solvents. Color changes visible to the naked eye were seen when AZM formed soluble and solid products with iodine. This type of color change is indicative of a strong CT interaction. UV–visible and Raman spectroscopies established that the CT interaction between AZM and iodine in the CH_2Cl_2, $CHCl_4$, and C_6H_5Cl solvents formed a tri-iodide complex formulated as $[AZM{\cdot}I^+]I_3^-$. The XRD and TEM experimental data support that that the AZM-I_2 complex prepared in all of the solvents possessed an amorphous structure composed of spherical particles 80 to 110 nm in size. The results obtained from this work provide the basis for future investigations into the CT interactions between AZM and other types of acceptors in addition to furnishing a big picture perspective on the CT chemistry of AZM.

Author contributions

A.M.A.A. and M.S.H. designed and observed the proposal and contributed to data analysis and interpretation. M.S.H. and A.M.A. performed the experiments. A.M.A.A. and H.A.S. surveyed the database and performed the spectral analysis. A.M.A.A. and M.S.H. provided conceptual advice and wrote the paper. All authors discussed the results and implications and commented on the manuscript at all stages.

Declaration of Competing Interest

The authors declare that no conflict of interest.

Acknowledgments

This work was funded by Taif University Researchers Supporting Project Number (TURSP-2020/02), Taif University, Taif, Saudi Arabia.

Appendix A. Supplementary data

Supplementary data to this article can be found online at https://doi.org/10.1016/j.molliq.2020.115187.

References

[1] R.S. Mulliken, W.B. Person, Molecular Complexes, Wiley, New York, 1969.
[2] R.S. Mulliken, J. Am. Chem. Soc. 72 (1950) 600.
[3] R. Foster, Organic Charge-Transfer Complexes, Academic Press, London, 1969.
[4] T. Madrakian, S. Heidari, Chin. Chem. Lett. 25 (2014) 1375.
[5] R.S. Mulliken, J. Phys. Chem. 56 (1952) 801.
[6] S.K. Das, G. Krishnamorthy, S.K. Dofra, Can. J. Chem. 78 (2000) 191.
[7] S. Shakya, I.M. Khan, J. Hazard. Mater. 403 (2021) 123537.
[8] A.S. Al-Attas, M.M. Habeeb, D.S. Al-Raimi, J. Mol. Liq. 148 (2–3) (2009) 58.
[9] J. Seliger, V. Zagar, K. Gotoh, H. Ishida, A. Konnai, D. Amino, T. Asaji, Phys. Chem. Chem. Phys. 11 (13) (2009) 2281.
[10] T. Asaji, Y. Yoshimura, D. Amino, Hyperfine Interact. 179 (1–3) (2007) 1.
[11] A.S. Gaballa, C. Wagner, S.M. Teleb, E.M. Nour, M.A.F. Elmosallamy, G.N. Kaluderovic, H. Schmidt, D. Steinborn, J. Mol. Struct. 876 (1–3) (2008) 301.
[12] T. Murata, Y. Morita, Y. Yakiyama, K. Fukui, H. Yarnochi, G. Saito, K. Nakasuji, J. Am. Chem. Soc. 129 (35) (2007) 10837.
[13] H. Suzuki, H. Mori, J.I. Yamaura, M. Matsuda, H. Tajima, T. Mochida, Chem. Lett. 36 (3) (2007) 402.
[14] S. Horiuchi, F. Ishii, R. Kumai, Y. Okimoto, H. Tachibana, H. Nagaosa, Y. Tokura, Nat. Mater. 4 (2005) 163.
[15] S. Horiuchi, R. Kumai, Y. Tokura, J. Am. Chem. Soc. 127 (2005) 5010.
[16] M. Amano, Y. Yamamura, M. Sumita, S. Yasazuka, H. Kawaji, T. Atake, K. Saito, J. Chem. Phys. 130 (2009), 034503, .
[17] G.G. Parra, A.L.S. Pavanelli, L.P. Franco, L.N.C. Máximo, R.S. da Silva, I. Borissevitch, J. Photochem. Photobiol. A 398 (2020) 112580.
[18] J. Li, X. Zhang, J. Nie, X. Zhu, J. Photochem. Photobiol. A 402 (2020), 112803, .
[19] S. Lee, J. Hong, S. Jung, K. Ku, G. Kwon, W.M. Seong, H. Kim, G. Yoon, I. Kang, K. Hong, H.W. Jang, K. Kang, Energy Storage Mater. 20 (2019) 462.
[20] Q. Wang, X. Bian, Z. Suo, Y. Han, H. Li, J. Lumin. 213 (2019) 530.
[21] M.V. Rusalov, V.V. Volchkov, V.L. Ivanov, M.Ya. Melnikov, F.E. Gostev, V.A. Nadtochenko, A.I. Vedernikov, S.P. Gromov, M.V. Alfimov, J. Photochem. Photobiol. A 372 (2019) 89.
[22] A.S.A. Almalki, A. Alhadhrami, A.M.A. Adam, I. Grabchev, M. Almeataq, J.Y. Al-Humaidi, T. Sharshar, M.S. Refat, J. Photochem. Photobiol. A 361 (2018) 76.
[23] A.S.A. Almalki, A. Alhadhrami, R.J. Obaid, M.A. Alsharif, A.M.A. Adam, I. Grabchev, M.S. Refat, J. Mol. Liq. 261 (2018) 565.
[24] A.S. Datta, S. Bagchi, A. Chakrabortty, S.C. Lahiri, Spectrochim. Acta A 146 (2015) 119.
[25] A.M.A. Adam, M.S. Refat, H.A. Saad, C.R. Chimie 18 (2015) 914.
[26] M. Saravanabhavan, K. Sathya, V.G. Puranik, M. Sekar, Spectrochim. Acta A 118 (2014) 399.
[27] H.M. Elqudaby, G.G. Mohamed, G.M.G. El-Din, Spectrochim. Acta A 129 (2014) 84.
[28] V. Murugesan, M. Saravanabhavan, M. Sekar, J. Photochem. Photobiol. B 140 (2014) 20.
[29] B. Kanci Bozoğlan, S. Tunç, O. Duman, J. Lumin. 155 (2014) 198.
[30] N. Singh, I.M. Khan, A. Ahmad, S. Javed, J. Mol. Struct. 1065-1066 (2014) 74.
[31] I.M. Khan, A. Ahmad, M.F. Ullah, Spectrochim. Acta A 102 (2013) 82.
[32] I.M. Khan, A. Ahmad, S. Kumar, J. Mol. Struct. 1035 (2013) 38.
[33] K. Sharma, S.P. Sharma, S.C. Lahiri, Spectrochim. Acta A 92 (2012) 212.
[34] D.K. Kuila, S.C. Lahiri, J. Soln. Chem. 41 (2012) 36.
[35] I.M. Khan, A. Ahmad, M.F. Ullah, J. Photochem. Photobiol. B 103 (2011) 42.
[36] I.M. Khan, A. Ahmad, M. Aatif, J. Photochem. Phtobiol. B: Biol. 105 (2011) 6.
[37] U.W. Rabie, M.H. Abou-El-Wafa, R.A. Mohamed, J. Mol. Struct. 871 (2007) 6.
[38] Y. Liang, W. Xing, L. Liu, Y. Sun, W. Xu, D. Zhu, Org. Electron. 78 (2020), 105608, .
[39] H.A. Hashem, M.S. Refat, Surf. Rev. Lett. 13 (2006) 439.
[40] D.K. Roy, A. Saha, A.K. Mukherjee, Spectrochim. Acta A 61 (2005) 2017.
[41] R.K. Gupta, R.A. Sing, J. Appl. Sci. 5 (2005) 28.
[42] M. Kidwai, S. Saxena, S. Rastogi, R. Venkataramaman, Curr. Med. Chem. Anti-Infective Agents 2 (2004) 269.
[43] A. Tracz, Pol. J. Chem. 76 (2002) 457.
[44] A. Dozal, H. Keyzer, H.K. Kim, W.W. Way, Int. J. Antimicrob. Agents 14 (2000) 261.
[45] T. Roy, K. Dutta, M.K. Nayek, A.K. Mukherjee, M. Banerjee, B.K. Seal, J. Chem. Soc. Perkin Trans. 2 (1999) 2219.
[46] F. Gutmann, C. Johnson, H. Keyzer, J. Molnar, Charge Transfer Complexes in Biochemistry Systems, Marcel Dekker Inc., 1992
[47] J. Feng, H. Zhong, B.D. Xuebau, Zir. Kexu 27 (6) (1991) 691.
[48] I.M. Khan, M. Islam, S. Shakya, K. Alam, N. Alam, M. Shahid, Bioorg. Chem. 99 (2020) 103779.
[49] I.M. Khan, S. Shakya, R. Akhtar, K. Alam, M. Islam, N. Alam, Bioorg. Chem. 100 (2020) 103872.
[50] S. Niranjani, K. Venkatachalam, J. Mol. Struct. 1219 (2020) 128564.
[51] V. Mahipal, N. Venkatesh, B. Naveen, G. Suresh, V. Manaiah, T. Parthasarathy, Chem. Data Collect. 28 (2020) 100474.
[52] A. Karmakar, P. Bandyopadhyay, S. Banerjee, N.C. Mandal, B. Singh, J. Mol. Liq. 299 (2020) 112217.
[53] R. Kavitha, S. Nirmala, R. Nithyabalaji, R. Sribalan, J. Mol. Struct. 1204 (2020) 127508.
[54] M.E. Mohamed, E.Y.Z. Frag, A.A. Hathoot, E.A. Shalaby, Spectrochim. Acta A 189 (2018) 357.
[55] O.R. Shehab, H. AlRabiah, H.A. Abdel-Aziz, G.A.E. Mostafa, J. Mol. Liq. 257 (2018) 42.
[56] G.G. Mohamed, M.M. Hamed, N.G. Zaki, M.M. Abdou, M.E. Mohamed, A.M. Abdallah, Spectrochim. Acta A 182 (2017) 143.
[57] O.A. Adegoke, C.P. Babalola, O.A. Kotila, O. Obuebhor, Arab. J. Chem. 10 (Supplement 2) (2017), S3848, .
[58] A.A. Sawsan, S.N. Nahla, F.M. Manal, A. Shimaa, E. Naglaa, Arab. J. Chem. 10 (Supplement 2) (2017), S1855, .
[59] N.B.S. Ismail, B. Narayana, JTUSCI 11 (5) (2017) 710.
[60] O.A. Adegoke, O.E. Thomas, S.N. Emmanuel, JTUSCI 10 (5) (2016) 651.
[61] S.A.M. Abdulrahman, O.Z. Devi, K. Basavaiah, K.B. Vinay, JTUSCI 10 (1) (2016) 80.
[62] N. Rahman, S. Sameen, M. Kashif, J. Mol. Liq. 222 (2016) 944.
[63] T.S. Belal, D.S. El-Kafrawy, M.S. Mahrous, M.M. Abdel-Khalek, A.H. Abo-Gharam, Spectrochim. Acta A 155 (2016) 47.
[64] A.A. Gouda, M. Kasssem, Arab. J. Chem. 9 (Supplement 2) (2016), S1712, .
[65] N.Z. Alzoman, J.M. Alshehri, I.A. Darwish, N.Y. Khalil, H.M. Abdel-Rahman, Saudi Pharm. J. 23 (1) (2015) 75.
[66] H.M. Elqudaby, G.G. Mohamed, G.M.G. El-Din, Spectrochim. Acta A 129 (2014) 84.
[67] T.A. Altalhi, J. Mol. Liq. 300 (2020) 112325.
[68] M.T. Basha, R.M. Alghanmi, S.M. Soliman, W.J. Alharby, J. Mol. Liq. 309 (2020) 113210.
[69] P.S. Koroteev, A.B. Ilyukhin, K.A. Babeshkin, N.N. Efimov, J. Mol. Struct. 1207 (2020) 127800.
[70] A. El-Dissouky, T.E. Khalil, H.A. Elbadawy, D.S. El-Sayed, A.A. Attia, S. Foro, J. Mol. Struct. 1200 (2020) 127066.
[71] F.A. Al-Saif, A.A. El-Habeeb, M.S. Refat, H.H. Eldaroti, Abdel Majid A. Adam, H. Fetooh, H.A. Saad, J. Mol. Liq. 293 (2019), 111517, .
[72] F.A. Al-Saif, A.A. El-Habeeb, M.S. Refat, Abdel Majid A. Adam, H.A. Saad, A.I. El-Shenawy, H. Fetooh, J. Mol. Liq. 287 (2019), 110981, .
[73] N. Venkatesh, B. Naveen, A. Venugopal, G. Suresh, V. Mahipal, P. Manojkumar, T. Parthasarathy, J. Mol. Struct. 1196 (2019) 462.

[74] U. Neupane, M. Singh, P. Pandey, R.N. Rai, J. Mol. Struct. 1195 (2019) 131.
[75] W. Falek, R. Benali-Cherif, L. Golea, S. Samai, N. Benali-Cherif, E. Bendeif, I. Daoud, J. Mol. Struct. 1192 (2019) 132.
[76] M. Faizan, Z. Afroz, M.J. Alam, V.H. Rodrigues, S. Ahmed, A. Ahmad, J. Mol. Struct. 1177 (2019) 229.
[77] K.S. Fathima, M. Sathiyendran, K. Anitha, J. Mol. Struct. 1176 (2019) 238.
[78] S. Soltani, P. Magri, M. Rogalski, M. Kadri, J. Mol. Struct. 1175 (2019) 105.
[79] L. Man, T. Li, X. Wu, K. Lu, L. Yang, X. Liu, Z. Yang, J. Zhou, C. Ni, J. Mol. Struct. 1175 (2019) 971.
[80] K. Ganesh, C. Balraj, A. Satheshkumar, K.P. Elango, Arab. J. Chem. 12 (2019) 503.
[81] V.V. Volchkov, M.N. Khimich, M.V. Rusalov, F.E. Gostev, I.V. Shelaev, V.A. Nadtochenko, A.I. Vedernikov, S.P. Gromov, A.Ya. Freidzon, M.V. Alfimov, M.Ya. Melnikov, Photochem. Photobiol. Sci. 18 (2019) 232.
[82] Y. Fu, Q. Xu, Q. Li, M. Li, C. Shi, Z. Du, ChemistryOpen 8 (2019) 127.
[83] A.K. Jeevan, K.R. Gopidas, Chem.Sel. 4 (2019) 506.
[84] Z. Afroz, M. Faizan, M.J. Alam, V.H.N. Rodrigues, S. Ahmad, A. Ahmad, J. Mol. Struct. 1171 (2018) 438.
[85] A. Karmakar, B. Singh, J. Mol. Struct. 1164 (2018) 404.
[86] L. Miyan, A. Ahmad Zulkarnain, J. Mol. Liq. 262 (2018) 514.
[87] R.M. Alghanmi, S.M. Soliman, M.T. Basha, M.M. Habeeb, J. Mol. Liq. 256 (2018) 433.
[88] K. Alam, I.M. Khan, Org. Electron. 63 (2018) 7.
[89] I.M. Khan, S. Shakya, N. Singh, J. Mol. Liq. 250 (2018) 150.
[90] S. Soltani, P. Magri, M. Rogalski, M. Kadri, Spectrochim. Acta A 205 (2018) 170.
[91] T. Chaudhuri, S. Santra, S. Jana, A. Hajra, Spectrochim. Acta A 204 (2018) 403.
[92] K.M. Al-Ahmary, M.M. Habeeb, A.H. Al-Obidan, Spectrochim. Acta A 196 (2018) 247.
[93] A. Karmakar, B. Singh, J. Mol. Liq. 247 (2017) 425.
[94] A. Karmakar, B. Singh, J. Mol. Liq. 236 (2017) 135.
[95] A.S.A. Almalki, A.M. Naglah, M.S. Refat, M.S. Hegab, A.M.A. Adam, M.A. Al-Omar, J. Mol. Liq. 233 (2017) 292.
[96] L. Miyan, S. Qamar, A. Ahmad, J. Mol. Liq. 225 (2017) 713.
[97] K.M. Al-Ahmary, S.M. Soliman, R.A. Mekheimer, M.M. Habeeb, M.S. Alenezi, J. Mol. Liq. 231 (2017) 602.
[98] R. Thirumurugan, K. Anitha, J. Mol. Struct. 1146 (2017) 273.
[99] I.M. Zulkarnain, A. Khan, L. Ahmad, M. Miyan, N. Azizc Ahmad, J. Mol. Struct. 1141 (2017) 687.
[100] V. Ulagendran, P. Balu, V. Kannappan, R. Kumar, S. Jayakumar, J. Mol. Struct. 1141 (2017) 213.
[101] P. Gogoi, U. Mohan, M.P. Borpuzari, A. Boruah, S.K. Baruah, J. Mol. Struct. 1131 (2017) 114.
[102] F. Ghasemi, K. Ghasemi, A.R. Rezvani, A. Shokrollahi, M. Refahi, S. García-Granda, R. Mendoza-Meroño, J. Mol. Struct. 1131 (2017) 30.
[103] N. Singh, A. Ahmad, J. Mol. Struct. 1127 (2017) 257.
[104] S. Özgün, E. Asker, O. Zeybek, J. Mol. Struct. 1127 (2017) 31.
[105] A. Karmakar, B. Singh, Spectrochim. Acta A 179 (2017) 110.
[106] M.S. Refat, A.M.A. Adam, M.Y. El-Sayed, Arab. J. Chem. 10 (2017) S3482.
[107] P. Misra, S. Badoga, A. Chenna, A.K. Dalai, J. Adjaye, Chem. Eng. J. 325 (2017) 176.
[108] L. Zulkarnain, A. Miyan, M.F. Ahmad, H. Alam, J. Younus, Photochem. Photobiol. B 174 (2017) 195.
[109] A.M.A. Adam, M.S. Refat, M.S. Hegab, H.A. Saad, J. Mol. Liq. 224 (2016) 311.
[110] K.M. Al-Ahmary, M.S. Alenezi, M.M. Habeeb, J. Mol. Liq. 220 (2016) 166.
[111] N. Rahman, S. Sameen, M. Kashif, J. Mol. Liq. 222 (2016) 944.
[112] N. Singh, I.M. Khan, A. Ahmad, S. Javed, J. Mol. Liq. 221 (2016) 111.
[113] A.M.A. Adam, M.S. Refat, J. Mol. Liq. 219 (2016) 377.
[114] L. Miyan, A. Ahmad, J. Mol. Liq. 219 (2016) 614.
[115] A.M.A. Adam, M.S. Refat, H.A. Saad, M.S. Hegab, J. Mol. Liq. 216 (2016) 192.
[116] H.S. El-Sheshtawy, M.M. Ibrahim, M.R.E. Aly, M. El-Kemary, J. Mol. Liq. 213 (2016) 82.
[117] S. Berto, E. Chiavazza, V. Ribotta, P.G. Daniele, C. Barolo, A. Giacomino, D. Vione, M. Malandrino, Spectrochim. Acta A 149 (2015) 75.
[118] N. Singh, I.M. Khan, A. Ahmad, S. Javed, J. Mol. Liq. 191 (2014) 142.
[119] N. Singh, A. Ahmad, J. Mol. Struct. 1074 (2014) 408.
[120] W. Chen, B. Huang, S. Ni, Y. Xiong, A.L. Rogach, Y. Wan, D. Shen, Y. Yuan, J. Chen, M. Lo, C. Cao, Z. Zhu, Y. Wang, P. Wang, L. Liao, C. Lee, Adv. Funct. Mater. (2019) 1903112.
[121] K. Medjanik, H. Elmers, G. Schönhense, J. Pouget, R. Valenti, M. Lang, Phys. Status Solidi B 256 (9) (2019), 1800745, https://doi.org/10.1002/pssb.201800745.
[122] J. Han, D. Yang, X. Jin, Y. Jiang, M. Liu, P. Duan, Angew. Chem. Int. Ed. 58 (2019) 7013.
[123] S. Lee, J. Hong, S. Jung, K. Ku, G. Kwon, W.M. Seong, H. Kim, G. Yoon, I. Kang, K. Hong, H.W. Jang, K. Kang, Energy Storage Mater. 20 (2019) 462.
[124] T. Salzillo, N. Crivillers, M. Mas-Torrent, K. Wurst, J. Veciana, Synth. Met. 247 (2019) 144.
[125] X. Chen, H. Wang, B. Wang, Y. Wang, X. Jin, F. Bai, Org. Electron. 68 (2019) 35.
[126] G. Kang, S. He, H. Cheng, X. Ren, J. Photochem. Photobiol. A 383 (2019) 111979.
[127] L. Meng, F. Chen, F. Bai, B. Bai, H. Wang, M. Li, J. Photochem. Photobiol. A 377 (2019) 309.
[128] Z. Zhao, Y. Duan, Q. Pan, Y. Gao, Y. Wu, Y. Geng, L. Zhao, M. Zhang, Z. Su, J. Photochem. Photobiol. A 375 (2019) 1.
[129] H. Sun, A. Khan, R. Usman, M. Wang, J. Photochem. Photobiol. A 371 (2019) 315.
[130] L. Man, T. Li, X. Wu, K. Lu, L. Yang, X. Liu, Z. Yang, J. Zhou, C. Ni, J. Mol. Struct. 1175 (2019) 971.
[131] S. Ghosh, B. Pramanik, D. Das, ChemNanoMat 4 (2018) 867.
[132] A. Firth, P. Prathapan, Eur. J. Med. Chem. 207 (2020) 112739.
[133] P. Zarogoulidis, N. Papanas, I. Kioumis, E. Chatzaki, E. Maltezos, K. Zarogoulidis, Eur. J. Clin. Pharmacol. 68 (5) (2012) 479.
[134] J. Min, Y.J. Jang, Med. Inf. 2012 (2012) 649570.
[135] I. Grgičević, I. Mikulandra, M. Bukvić, M. Banjanac, V. Radovanović, I. Habinovec, B. Bertoša, P. Novak, Int. J. Antimicrob. Agents (2020) 106147, https://doi.org/10.1016/j.ijantimicag.2020.106147.
[136] N. Zhu, D. Zhang, W. Wang, X. Li, B. Yang, J. Song, X. Zhao, B. Huang, W. Shi, R. Lu, P. Niu, F. Zhan, X. Ma, D. Wang, W. Xu, G. Wu, G.F. Gao, D. Phil, W. Tan, N. Engl. J. Med. 382 (2020) 727.
[137] Organization WH, WHO director-General's Opening Remarks at the Media Briefing on COVID-19, 11 March 2020, Geneva, Switzerland, 2020.
[138] I. Ali, O.M.L. Alharbi, Sci. Total Environ. 728 (2020) 138861.
[139] N. Bakhshaliyev, M. Uluganyan, A. Enhos, E. Karacop, R. Ozdemir, J. Electrocardiol. 62 (2020) 59.
[140] P. Gautret, J. Lagier, P. Parola, V.T. Hoang, L. Meddeb, M. Mailhe, B. Doudier, J. Courjon, V. Giordanengo, V.E. Vieira, H.T. Dupont, S. Honoré, P. Colson, E. Chabrière, B. La Scola, J. Rolain, P. Brouqui, D. Raoult, Int. J. Antimicrob. Agents 56 (2020) 105949.
[141] A. Pain, M. Lauriola, A. Romandini, F. Scaglione, Int. J. Antimicrob. Agents 56 (2020) 106053.
[142] S.M. Vouri, T.N. Thai, A.G. Winterstein, Res. Soc. Adm. Pharm. (2020)https://doi.org/10.1016/j.sapharm.2020.04.031.
[143] R.L. Mitra, S.A. Greenstein, L.M. Epstein, HeartRhythm Case Reports 6 (5) (2020) 244.
[144] S. Arshad, P. Kilgore, Z.S. Chaudhry, G. Jacobsen, D.D. Wang, K. Huitsing, I. Brar, G.J. Alangaden, M.S. Ramesh, J.E. McKinnon, W. O'Neill, M. Zervos, Int. J. Infect. Dis. 97 (2020) 396.
[145] F. Cataldo, Polym. Degrad. Stab. 176 (2020) 109155.
[146] X. He, X. Yi, F. Yin, B. Chen, G. Li, H. Yin, Electrochim. Acta 337 (2020) 135825.
[147] S.K. Kodadi, S. Kovuri, J. Mol. Struct. 1202 (2020) 127271.
[148] K. Tashiro, M. Gakhutishvili, Polymer 171 (2019) 140.
[149] H.T. Nguyen, D.D. Nguyen, J. Spanget-Larsen, Chem. Phys. Lett. 716 (2019) 119.
[150] P. Gogoi, U. Mohan, M.P. Borpuzari, A. Boruah, S.K. Baruah, Arab. J. Chem. 12 (2019) 4522.
[151] M.C. Divyasree, K. Vasudevan, K.K. Abdul Basith, P. Jayakrishnan, M.T. Ramesan, K. Chandrasekharan, Opt. Laser Technol. 105 (2018) 94.
[152] A.J.A. Baskar, A.S. Rajpurohit, M. Panneerselvam, M. Jaccobb, D.R. Singh, V. Kannappan, Chem. Data Collect. 7-8 (2017) 80.
[153] V. Ulagendran, P. Balu, V. Kannappan, R. Kumar, S. Jayakumar, J. Mol. Struct. 1141 (2017) 213.
[154] P. Gogoi, U. Mohan, M.P. Borpuzari, A. Boruah, S.K. Baruah, J. Mol. Struct. 1131 (2017) 114.
[155] S.A.M. Abdulrahman, O.Z. Devi, K. Basavaiah, K.B. Vinay, J. Taibah Univ. Sci. 10 (2016) 80.
[156] R. Kumar, A.J.A. Baskar, V. Kannappan, D. RoopSingh, J. Mol. Liq. 196 (2014) 404.
[157] N. Mandoumi, F. Nasri, M. Shariati-Rad, A. Taherpour, M.B. Gholivand, M. Shamsipur, J. Mol. Struct. 1047 (2013) 179.
[158] K. Ganesh, K.P. Elango, Spectrochim. Acta A 93 (2012) 185.
[159] K. Ganesh, C. Balraj, K.P. Elango, Spectrochim. Acta A 79 (2011) 1621.
[160] N. Alizadeh, S. Dehghanikhah, Chin. Chem. Lett. 22 (2011) 587.
[161] M. Pandeeswaran, K.P. Elango, Spectrochim. Acta A 75 (2010) 1462.
[162] M. Pandeeswaran, K.P. Elango, Spectrochim. Acta A 72 (2009) 789.
[163] S.K. Singh, R.K. Gupta, R.A. Singh, Synth. Met. 159 (2009) 2478.
[164] M. Pandeeswaran, E.H. El-Mossalamy, K.P. Elango, Int. J. Chem. Kinet. 41 (12) (2009) 787.
[165] G. Khayatian, F.S. Karoonian, J. Chin. Chem. Soc. 55 (5) (2008) 1042.
[166] G. Khayatian, H. Rezatabar, F.S. Karoonian, A. Salimi, J. Chin. Chem. Soc. 53 (5) (2006) 1133.
[167] M.R. Ganjali, S. Shirvani-Arani, G.N. Bidhendi, J. Chin. Chem. Soc. 53 (2) (2006) 275.
[168] K.S. Kumar, T. Parthasarathy, J. Solut. Chem. 46 (2017) 1364.
[169] D.A. Skoog, Principle of Instrumental Analysis, third ed. Saunders, New York, USA, 1985 (Chapter 7).
[170] M.S. Refat, H.A. Saad, A.M.A. Adam, Spectrochim. Acta A 141 (2015) 202.
[171] M.S. Refat, A.M.A. Adam, T. Sharshar, H.A. Saad, H.H. Eldaroti, Spectrochim. Acta A 122 (2014) 34.
[172] A.M.A. Adam, M.S. Refat, H.A. Saad, J. Mol. Struct. 1051 (2013) 144.
[173] A.M.A. Adam, M.S. Refat, T. Sharshar, Z.K. Heiba, Spectrochim. Acta A 95 (2012) 458.
[174] H.A. Benesi, J.H. Hildebrand, J. Am. Chem. Soc. 71 (1949) 2703.
[175] A.M. Hindawey, A.M.G. Nassar, R.M. Issa, Y.M. Issa, Indian J. Chem. 19A (1980) 27.
[176] Y.M. Issa, A.M. Hindawey, A.E. El-Kholya, R.M. Issa, Gazz. Chim. Ital. 111 (1981) 27.
[177] M. El-Sayed, S. Agrawl, Talanta 29 (1982) 535.
[178] A.N. Martin, J. Swarbrick, A. Cammarata, Physical Pharmacy, 3rd ed. Lee and Febiger, Philadelphia, PA, 1969 344.
[179] G. Briegleb, J. Czekalla, Z. Physikchem. (Frankfurt) 24 (1960) 237.
[180] G. Briegleb, Z. Angew. Chem. 72 (1960) 401.
[181] G. Aloisi, S. Pignataro, J. Chem. Soc. Faraday Trans. 69 (1973) 534.
[182] I. Isenberg, S.L. Baird, Solvent effects in radical ion formation, J. Am. Chem. Soc. 84 (1962) 3803.
[183] H. Tsubumora, R Lang, J. Am. Chem. Soc. 83 (1961) 2085.
[184] A.B.P. Lever, Inorganic Electronic Spectroscopy, second ed. Elsevier, Amsterdam, 1985.
[185] C. Balraj, K. Ganesh, K.P. Elango, J. Mol. Struct. 998 (2011) 110.
[186] M. Pandeeswaran, K.P. Elango, Spectrochim. Acta A 65 (2006) 1148.
[187] G. Varsanyi, Assignments for Vibrational Spectra of Seven Hundred Benzene Derivatives, vol. 1 and 2, Academic Kiado, Budapest, 1973.
[188] D.N. Sathyanarayana, Vibrational Spectroscopy- Theory and Applications, second ed New Age International (P) Limited Publishers, New Delhi, 2004.

[189] C. Sridevi, G. Velraj, J. Mol. Struct. 1019 (2012) 50.
[190] G. Socrates, Infrared and Raman Characteristic Group Frequencies-Tables and Charts, Third ed. Wiley, New York, 2001.
[191] D. Sajan, J. Binoy, B. Pradeep, K.V. Krishnan, V.B. Kartha, I.H. Joe, V.S. Jayakumar, Spectrochim. Acta A 60 (2004) 173.
[192] A.G. Maki, R. Forneris, Spectrochim. Acta A 23 (1967) 867.
[193] B. Karthikeyan, Spectrochim. Acta A 64 (2006) 1083.
[194] R.M. Silverstein, F.X. Webster, Spectrometric Identification of Organic Compounds, sixth ed. Jon Wiley Sons Inc., New York, 1963.
[195] W. Kiefer, H.J. Bernstein, Chem. Phys. Lett. 16 (1972) 5.
[196] L. Andrews, E.S. Prochaska, A. Loewenschuss, Inorg. Chem. 19 (1980) 463.
[197] K. Kaya, N. Mikami, Y. Udagawa, M. Ito, Chem. Phys. Lett. 16 (1972) 151.
[198] E.M. Nour, L.H. Chen, J. Lanne, J. Phys. Chem. 90 (1986) 2841.
[199] E.M. Nour, L.A. Shahada, Spectrochim. Acta A 45 (1989) 1033.
[200] M.S. Refat, A.M.A. Adam, H.A. Saad, A.M. Naglah, M.A. Al-Omar, Int. J. Electrochem. Sci. 10 (2015) 6405.
[201] E.M. El-Neema, Spectrochim. Acta A 60 (2004) 3181.
[202] M. Pandeeswaran, K.P. Elango, J. Solut. Chem. 38 (12) (2009) 1558.